Nonergodic dynamics for an impurity interacting with bosons in a tilted lattice

Pedro R. Nicácio Falcão[1,2] and Jakub Zakrzewski[2,3,*]

[1]*Szkoła Doktorska Nauk Ścisłych i Przyrodniczych, Uniwersytet Jagielloński, Łojasiewicza 11, PL-30-348 Kraków, Poland*

[2]*Instytut Fizyki Teoretycznej, Wydział Fizyki, Astronomii i Informatyki Stosowanej, Uniwersytet Jagielloński, Łojasiewicza 11, PL-30-348 Kraków, Poland*

[3]*Mark Kac Complex Systems Research Center, Uniwersytet Jagielloński, PL-30-384 Kraków, Poland*

(Received 15 June 2023; revised 21 August 2023; accepted 2 October 2023; published 17 October 2023)

The fate of a single particle immersed in and interacting with a bath of other particles localized in a tilted lattice is investigated. For tilt values comparable to the tunneling rate a slow-down of the dynamics is observed without, however, a clear localization of the impurity. For a large tilt and strong interactions the motion of the impurity resembles that in the Kronig-Penney potential. The dynamics of the impurity depends on the initial distribution of majority particles. It shows delocalized dynamics for a regular, density-wave-like distribution and localization if majority particles are randomly distributed.

DOI: 10.1103/PhysRevB.108.134201

I. INTRODUCTION

Studies of a small impurity interacting with the medium it is immersed in have a long history. The modern formulation dates back to Landau [1], who considered the motion of an electron in a dielectric crystal. Due to interactions, the electron dresses in the phonon cloud forming a complex object—a polaron—named and studied by Solomon Pekar [2–5]. More modern studies have considered an impurity interacting with seas of ultracold bosons [6–16] or fermions [17–24]. The motion of an impurity in the Bose-Einstein condensate may be considered as an example of a quantum walk [25–36].

Recently, the study of an impurity interacting with a disordered medium received significant attention. Delocalization of a particle, in the presence of disorder, due to an additional coupling to a bath [37–42] was studied in a variety of situations. A single impurity interacting with the Anderson-localized medium was considered in detail in Refs. [43–46]. Small system studies indicated impurity induced delocalization for small disorder [43], while studies of larger systems at large disorder indicated localization at short times [44,45]. However, it was shown that this conclusion must be treated with caution when longer interaction times were considered [46]. The latter study extended the analysis to the quasiperiodic disorder.

The aim of the present work is to consider the dynamics of an impurity interacting with majority particles in a one-dimensional tilted lattice. This problem is disorder-free, yet recent studies have shown that known Stark localization for noninteracting particles extends also to the interacting case [47–56]. Both the spectral statistics (such as gap ratio [57,58]) as well the as time dynamics reveal significant similarities between disorder-induced or tilt-induced localization. It is interesting, therefore, to see whether the motion of the impurity in disordered and tilted lattices also reveals common features. Some differences may be expected because it is well known that localization may be vulnerable to external perturbations, e.g., a coupling to additional phononic [37] or bosonic baths [41]. Here the impurity may be considered [44,45] to be a very small bath perturbing the Anderson- or Stark-localized system. Often, in such situations one may observe subdiffusive transport [39,42].

The paper is organized as follows: In Sec. II we describe the model studied as well as define observables that we use to characterize the system. Section III describes the results obtained for a relatively small system with the Hamiltonian exponentiation approach [59,60] that allows us to analyze long-time behavior while in Sec. IV we consider larger systems using a variational approach based on tensor networks. Both approaches are compared briefly in the Appendix. Section V considers the role of random positional disorder in the initial state for the dynamics—here we consider larger systems only. We conclude in Sec. VI.

II. THE MODEL AND METHODS

We consider two species of hard-core bosons residing in a common one-dimensional lattice with open boundary conditions described by the Hamiltonian:

$$H = J\sum_{i=1}^{L-1}(\hat{d}_i^\dagger \hat{d}_{i+1} + \text{H.c.}) + \sum_{i=1}^{L} h_i \hat{n}_{d,i} + J\sum_{i=1}^{L-1}(\hat{c}_i^\dagger \hat{c}_{i+1} + \text{H.c.}) + U\sum_{i=1}^{L}\hat{n}_{c,i}\hat{n}_{d,i}, \quad (1)$$

where J denotes the tunneling amplitude assumed, for simplicity, to be the same for both c and d species (later on we fix the units with $J = \hbar = 1$). $\hat{d}_i$, $\hat{d}_i^\dagger$ ($\hat{c}_i$, $\hat{c}_i^\dagger$) are the annihilation and creation operators for d (c) bosons at site i, while $\hat{n}_{d,i}$ ($\hat{n}_{c,i}$) are their occupation number operator at site i. The interaction

*jakub.zakrzewski@uj.edu.pl

strength between the two species is characterized by U, while the on-site chemical potential acting on the d particles is characterized by h_i. A single-c particle does not feel any potential and it would move freely for $U = 0$. We shall study how the interactions with d particles affect the c-impurity dynamics and how the presence of the impurity affects the d particles.

A similar model was introduced in Refs. [44,45], where it was assumed that h_i is randomly and uniformly distributed, $h_i \in [-W, W]$, resulting in Anderson localization for d particles alone. While short-time study [44,45,61] hinted at the appearance of many-body localization (MBL) in the system for sufficiently large interactions U between d particles and c and appropriately chosen disorder amplitude W, the study of longer times showed that MBL-like behavior is rather a transient effect and the impurity spreads subdiffusively in the system, leading also to the slow delocalization of d species [46].

Let us underline that the hard-core bosons model maps to spin 1/2 system (with an empty site corresponding to the spin-down state while the occupied site to the spin-up state or vice versa). Those in turn, via the Jordan-Wigner transformation, may be transformed into spinless fermions. Thus the model, (1) is quite general. The hard-core assumption arises in cold atomic physics when the on-site interaction among particles is huge. Then the double (or higher) occupancy on a given site is energetically very costly and the motion of particles may be restricted to a single occupancy subspace. Such an approach is widely utilized in studies of dynamical and ground-state properties of, e.g., dipolar systems [62–64]. Also the impurity localization problem in hard-core boson models has been studied in prior works [44–46].

In our study we shall use a similar set of parameters as Refs. [44–46], concentrating, in particular, on $U = 12$ case, but we shall replace the random uniform disorder with a constant tilt of the lattice $h_i = Fi$. Also, we use similar approximate numerical approach to study time dynamics, i.e., the time-dependent variational principle (TDVP) technique with matrix product states. Specifically, we follow the prescription given in Refs. [65,66] and use a combination of two-site and one-site codes, for details see Ref. [46]. For small system sizes, up to $L = 24$, we use also the exact time propagation as supplied by the QuSpin code [59,60] comparing its results with that of TDVP propagation for similar system sizes in the Appendix.

Note that the Hamiltonian (1) is particle-hole symmetric so the motion of a single c impurity in the presence of $\overline{n}$ filling of d bosons will be the same as for $1 - \overline{n}$ filling. For this reason, we consider two filling cases. Inspired by Refs. [44–46] we consider first the 1/3 filling of d bosons prepared in a Fock, charge-density wave-like state, i.e., $|0, 1, 0, 0, 1, 0, 0, \ldots\rangle$. Those particles, in the presence of a constant lattice tilt, undergo Wannier-Stark localization. Next, we discuss the 1/2 filling with d particles being in the $|1, 0, 1, 0 \ldots\rangle$ initial state that leads to stronger interactions for the same U. Finally, we consider the situation when d particles are randomly distributed, introducing the positional disorder. In all cases, a single c boson is placed in the middle of the chain at the site i_0 which is initially empty. Its spreading in the lattice is affected by the interaction with d particles.

Note that it is also possible to place the impurity in the site already occupied by the d particle. This, however, shifts the energy of the system by a large value of U, so the system is strongly perturbed by the impurity. The tunneling from such a state is strongly nonresonant slowing down considerably the initial time evolution.

The full dimension of the Hilbert space for our problem is

$$\dim\mathcal{H} = L \times \binom{L}{N_d}, \tag{2}$$

with the first term corresponding to the Hilbert-space dimension of the impurity c and the second term associated with the number of d-type hard-core bosons (or fermions), N_d. The filling is, therefore, $\overline{n} = N_d/L$. In the following, we present the "exact" numerical data for L around 20, which corresponds to the Hilbert-space dimension of the order of a few million. For larger systems, of the order of $L = 60$, we use an approximate TDVP algorithm based on matrix product states (MPSs) (for details see the Appendix and Ref. [46]).

We consider the following observables: The impurity density, $n_{c,i}(t) = \langle \hat{n}_{c,i}(t)\rangle$, which reveals a possible spreading of the c boson through the chain, and the density of the background bosons affected by the tilt of the lattice, $n_{d,i}(t) = \langle \hat{n}_{d,i}(t)\rangle$. We find that useful information is provided by the mean square deviation (MSD) for the c boson position defined as

$$\mathrm{MSD}(t) = \sum_i^L n_{c,i}(i - i_0)^2 - \left(\sum_i^L n_{c,i}(i - i_0)\right)^2. \tag{3}$$

The MSD is similar to the quantity studied in Refs. [67,68] in the context of MBL. The diffusive spread is indicated by a linear growth $\mathrm{MSD}(t) \propto t$. A saturation after an initial growth is a hallmark of Anderson localization. It is believed [67,68] that the growth of MSD in a genuine many-body interacting system in the MBL phase is slower than any power in time and persists for a long time.

Additionally, we consider the time correlation function of d particles defined as

$$C_d(t, L_b) = \sum_{l=L_b+1}^{L-L_b} [n_{d,l}(t) - \overline{n}][n_{d,l}(0) - \overline{n}], \tag{4}$$

where $\overline{n}$, the mean density which, for our initial state, is typically $\overline{n} = 1/3$. L_b denotes the number of sites on both edges of the chain removed from the correlation function. To avoid boundary effects we take $L_b = 3$. If the memory of the initial state is lost, $n_{d,l}(t)$ should reach $\overline{n}$ at all sides leading to vanishing $C_d(t, L_b)$.

We analyze also the entropy of entanglement by splitting the system on the i-bond into two subsystems A and B with A containing the first i sites. This allows us, in principle, to test whether the logarithmic entropy growth, considered as another feature of MBL appears in the system studied. Let us define the density matrix for the subsystem A as $\rho_A(t) = \mathrm{Tr}_B|\psi(t)\rangle\langle\psi(t)|$ where $|\psi(t)\rangle$ is the quantum state of the system at a given time t. Then the entanglement entropy across this bond reads

$$\mathcal{S} = -\mathrm{Tr}[\rho_A \ln \rho_A] = -\sum_k \rho_k \ln \rho_k, \tag{5}$$

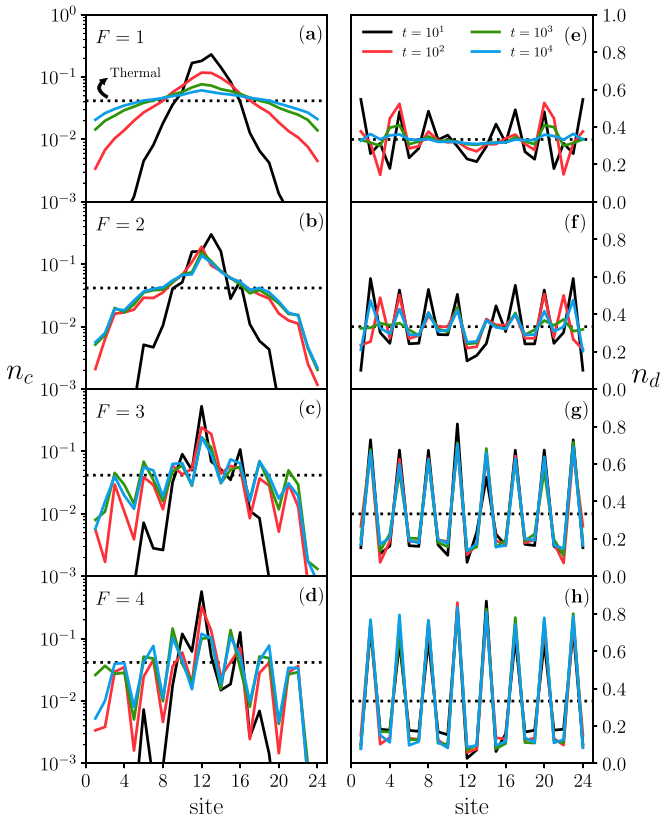

FIG. 1. Impurity density, n_c (left) and tilted hard-core bosons density, n_d (right) for different values of the tilt F, as indicated in the panels. The initial state of tilted bosons is $|010010\ldots010\rangle$, while the impurity is placed in an initially empty central site of $L = 24$ chain (total Hilbert-space dimension being 1.76×10^7). The interaction strength is $U = 12$. Dotted lines indicate equilibrium occupations.

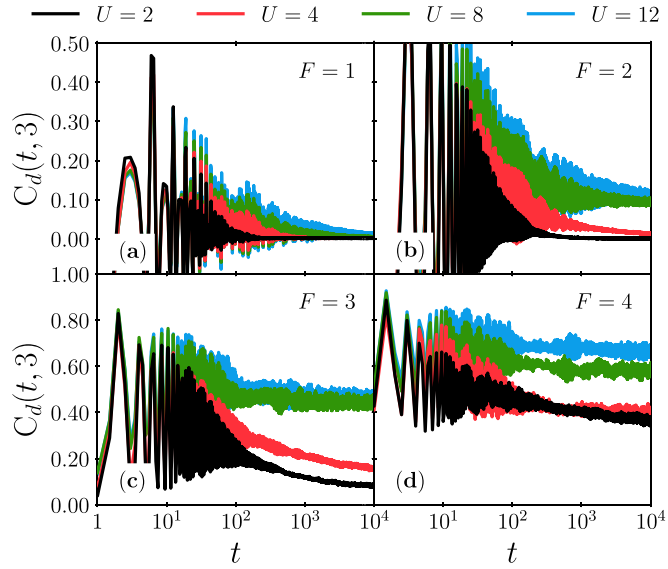

FIG. 2. Time dependence of the correlation function for d particles for different values of the interaction strength U (as indicated above in the figure), different tilt values (indicated in the panels), and $L = 21$ chain shows that only for strong interactions does the motion remain nonergodic on the timescales considered. To avoid boundary effects, we drop $L_b = 3$ sites from both edges in the calculation of $C_d(t, L_b)$.

where ρ_k are the squares of the Schmidt basis coefficients fulfilling $\sum_k \rho_k = 1$ (see, e.g., Ref. [69]). Furthermore, we can split the entanglement entropy $\mathcal{S}$ into two parts [70]:

$$\mathcal{S} = \mathcal{S}_N + \mathcal{S}_C, \tag{6}$$

where $\mathcal{S}_N$ denotes the number (classical) entropy describing particle number fluctuations between A and B subsystems and $\mathcal{S}_C$ denotes the configurational (quantum) entropy (describing various particle configurations in A and B). Denote by p_n the probability of occupying the n-particle sector in A and by $\rho^{(n)}$ the corresponding block of the density matrix $\rho_A = \sum p_n \rho^{(n)}$. Then [70],

$$\mathcal{S}_C = -\sum_n p_n \mathrm{Tr}(\rho^{(n)} \ln \rho^{(n)}), \tag{7}$$

$$\mathcal{S}_N = -\sum_n p_n \ln p_n. \tag{8}$$

.

III. SMALL SYSTEM SIZES

We begin our analysis with systems of small sizes amenable to an exact time propagation. They allow us also to reach longer times of evolution. We consider 1/3 filling first. Figure 1 presents the time dynamics of both the impurity and the background bosons in the tilted lattices for different values of the tilt, F. We assume the interaction of c and d species to be quite high, $U = 12$, as in Refs. [44,45]. For a small tilt ($F = 1$), the impurity decays from the initial site and tends to spread over the whole lattice, suggesting a slow delocalization towards its thermal behavior. This tendency to an ergodic behavior can also be seen by looking at the density profile of the d-type bosons, where they lose completely the memory of their initial configuration, "melting" to $n_{d,i} = \overline{n}$. An interesting scenario emerges when we increase the magnitude of the tilt to $F = 2$. Despite an initial spread, the impurity density seems to freeze in a specific configuration, thus suggesting some sort of localization. This localized behavior is also reflected in the background bosons, which do not completely lose the memory of their initial configuration, even when the system is evolved for a very long time (up to $10^4 J^{-1}$).

This is confirmed by the time dependence of the correlation function, (4), shown in Fig. 2. Here we show the system dynamics for different interaction strengths, U. For smaller U values, the correlations, after initial oscillations, decay fast to zero indicating ergodic behavior. This is to be contrasted with large U, in particular the $U = 12$ case, where the oscillations of the correlation function decay slower and the asymptotic values (not reached even for long 10^4 times considered) seem to be nonzero, at least for the $F > 2$ cases. The oscillations are the remnants of Bloch oscillations, which would dominate the dynamics of d particles for $U = 0$.

The interesting, nonergodic dynamics therefore occurs for strong interactions, from now on we shall consider mostly the $U = 12$ case.

The hat-like behavior of the impurity density with the maximum at its original position, particularly visible for $F = 2$, suggests some sort of memory of the initial position of the

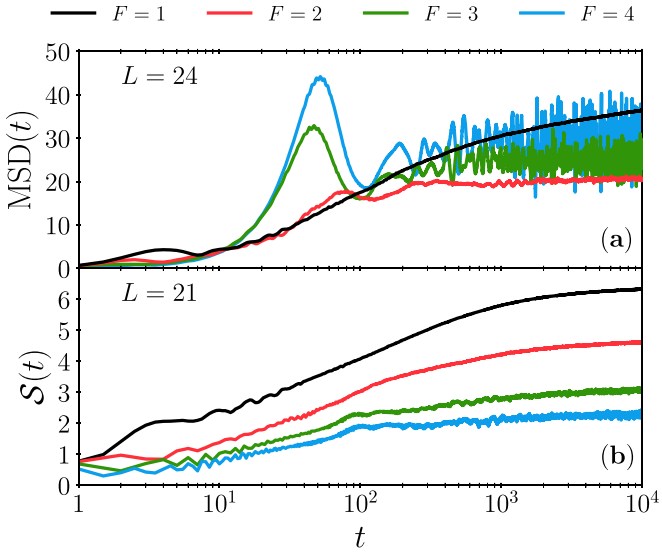

FIG. 3. (a) Mean square deviation MSD(t) time dependence for c-particle distribution for $U = 12$ and different values of F for system size $L = 24$. (b) Time dynamics of the entanglement entropy in the middle of the chain for slightly smaller system size, $L = 21$.

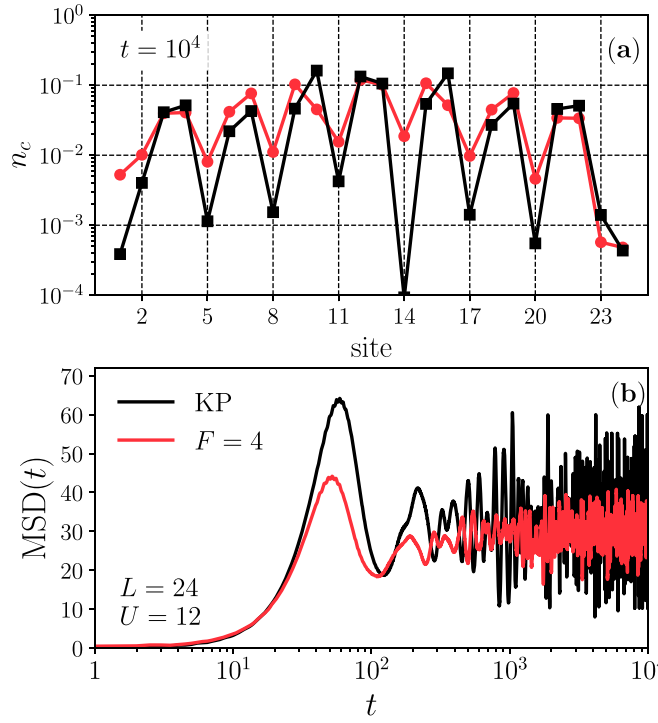

FIG. 4. Comparison of the exact dynamics and that generated by a static Kronig-Penney (KP) potential of amplitude $U = 12$, Eq. (9).

c particle. It is accompanied by a strong modification of the background d-boson distribution in this central position. This behavior persists at quite large times (up to $10^4 J^{-1}$) where both $n_{c,i}$ and $n_{d,i}$ seem to keep their shape, being extremely weakly dependent on time.

To provide a more quantitative picture of the impurity dynamics, Fig. 3 shows the growth of MSD, Eq. (3), for different F values and strong interactions. This growth necessarily reflects the trends that may be invoked from Fig. 1. For small $F = 1$ the wave packet apparently spreads quite fast, the spread slows down in time but does not stabilize on the timescale considered. Markedly different is the growth of MSD for the $F = 2$ case. The initial growth saturates around $t = 200$ and then remains practically constant with possibly a very slow growth. On the other hand, for still bigger tilt, $F = 3, 4$, one observes initially a fast superdiffusive growth ($\approx t^\alpha$ with $\alpha > 1$) of MSD which then stops growing but rather undergoes significant oscillations. By comparing the results obtained for different system sizes, not shown, one may verify that the time when the first maximum of MSD is formed is roughly proportional to the system size L and is related to the moment when the front of the wave packet reaches the edges of the system. At roughly the same time the entanglement entropy growth, Fig. 3(b), changes from a steep growth to a slow logarithmic-like behavior for $F = 3, 4$ while for smaller F values studied, the growth is substantially faster. Let us note that we report calculation of S for a slightly smaller system size, $L = 21$, since the corresponding calculations for $L = 24$ would require excessive computer time. Still, we show MSD in Fig. 3(a) for the largest L we could handle.

Let us leave aside for a moment the fast initial growth of MSD in the initial $t \in [0, 100]$ period. Clearly, the dynamics for $t > 100$ and larger values of F studied shows features expected for MBL: the distribution of c as well as d particles stabilizes in out-of-equilibrium configurations with a close to exponential distribution for c particles centered at its initial position (and revealing fast oscillations as visible from MSD fast changes at later times). Still, the mean value of MSD changes very slowly, following the MBL signature of Refs. [67,68]. The entanglement entropy shows a slow logarithmic-like growth, in agreement with another hallmark of MBL [71,72].

Can we somehow provide a physical understanding of this dynamics? An interesting picture emerges noting the fact that d particles for such large F values are practically localized at their initial positions. Suppose that they are strictly immobile. Then, they provide a periodic Kronig-Penney (KP) δ-type potential [73] of amplitude U for the motion of c particles. Then the effective Hamiltonian governing the motion of the c impurity is

$$H_{\text{eff}} = J \sum_{i=1}^{L-1} (\hat{c}_i^\dagger \hat{c}_{i+1} + \text{H.c.}) + U \sum_{i \in \mathcal{O}} \hat{n}_{c,i}, \tag{9}$$

where $\mathcal{O}$ is a set of sites occupied initially by d particles, i.e., $\mathcal{O} = \{2, 5, 8, \ldots\}$.

Such an asymptotic picture may only be approximate, as it does not depend on F value (still under the assumption that F is large). However, already in Fig. 3, the time dependence of MSD for $F = 3$ and $F = 4$ looks quite similar, Fig. 4 compares $F = 4$ case with the dynamics obtained with the Hamiltonian (9). The latter is a strictly periodic problem soluble by extended Bloch waves. Still, the fact that the potential acts only on every third site has pronounced consequences for the impurity dynamics. Notably, the occupation of sites remains nonuniform, with sites where the (repulsive) potential U is present being less occupied than other sites, observe the

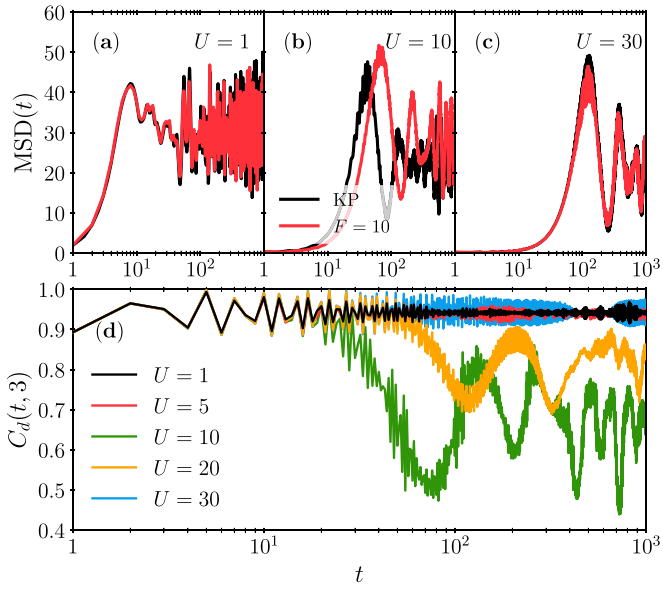

FIG. 5. Comparison of the exact dynamics with the KP approximate one for strong tilt, $F = 10$ and different U values. Observe that the deviations from KP approximation as well as a partial decorrelation of d particles is the strongest for resonance $F = U$ when the difference in energies between neighboring sites due to the tilt may be compensated by the interaction energy. Here the system size $L = 21$.

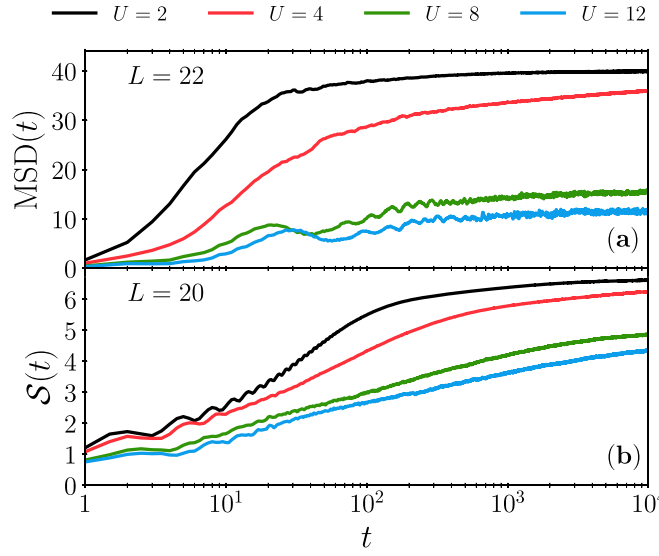

FIG. 6. The time dynamics at half filling. (a) Mean square deviation MSD(t) time dependence for c particle distribution for $F = 2$ and different values of U. (b) The corresponding time dynamics of the entanglement entropy in the middle of the chain for a slightly smaller size $L = 20$.

black squares in Fig. 4(a). This may be seen also in MSD(t) which undergoes fast oscillations (after the initial ballistic growth) around a value ($t \approx 30$).

Let us note that apparently the effective Hamiltonian explains the character of the fast growth of MSD for small times. It represents ballistic motion in the approximate KP potential.

Interestingly, in the presence of interactions, the MSD remains very similar to that obtained for the noninteracting case while the entanglement entropy dramatically changes. For a single particle in an immobile background, the entanglement entropy grows,reaching the value ln(2). This contribution comes solely from the number entropy, with the value emphasizing that the particle is either on the left or on the right of a given bond. In the interaction case the entanglement entropy grows fast initially until times of the order of hundred when the first bump in MSD occurs. Then the growth slows down and remains logarithmic up to the longest times (10^4) considered, as seen in Fig. 3(b). Thus, despite similarity with the noninteracting KP case in particle distributions, we observe here a hallmark of MBL—the logarithmic growth of the entanglement entropy.

The validity of the KP potential approximation depends also on U value. Consider a really strong $F = 10$ case. Figure 5 shows MSD and the correlation function of d particles for different U values. For both weak and strong interactions one observes that the KP approximate description works well for the impurity, also correlations between d particles are close to their original value. At resonance, $F = U$ (and in its vicinity) this picture partially breaks. When $F = U$ the difference of energies between neighboring sites due to the tilt is equal the interaction energy present if c and d particles meet at a given site. Thus locally the tunneling becomes resonant. This is, however, a local process and does not extend over many sites, thus leading to a partial decorrelation of d particles only. Large $U \gg F$ leads to almost impenetrable barriers of the KP potential, which slows down the dynamics, as seen by comparing time dynamics in top row of Fig. 5. At the same time a full correlation between d particles is preserved. Note that the timescale in Fig. 5 is up to $t = 10^3$ only because computer simulations for large F and U values are time costly.

Consider now, briefly, the "optimal" density of d particles, i.e. $\overline{n} = 1/2$. As an initial state we take a product state $|101010\cdots\rangle$. We observe a similar behavior to that for $\overline{n} = 1/3$. Figure 6 presents the MSD(t) and the corresponding entanglement entropy for different interaction strengths U and $F = 2$. For smaller U values a fast growth of both MSD and S indicates a lack of localization, while the data for $U = 12$, on the other side, show a very modest value of MSD with an almost logarithmic growth of the entanglement entropy. Note that while the data are obtained for $L = 22$ with the Hilbert-space dimension of 1.55×10^7, for the entanglement entropy dynamics we report the data for $L = 20$ with the corresponding dimension of 3.7×10^6.

We inspect again the $U = 12$ case, comparing now MSD for different F values shown in Fig. 7. While for large F we observe a similar behavior as for the smaller density—the MSD time dependence shows great similarity with results for the KP potential with frozen d particles, even for $F = 2$, MSD(t) grows slowly being accompanied by a similarly slow, logarithmic growth of the entanglement entropy. Thus increased effective interactions for half filling clearly favor MBL also for smaller tilt values. In particular, already for $F = 2$ we observe a (sub)logarithmic growth of the entanglement entropy. Importantly for that F value MSD grows also very slowly and is limited to low values indicating freezing of the corresponding time dynamics.

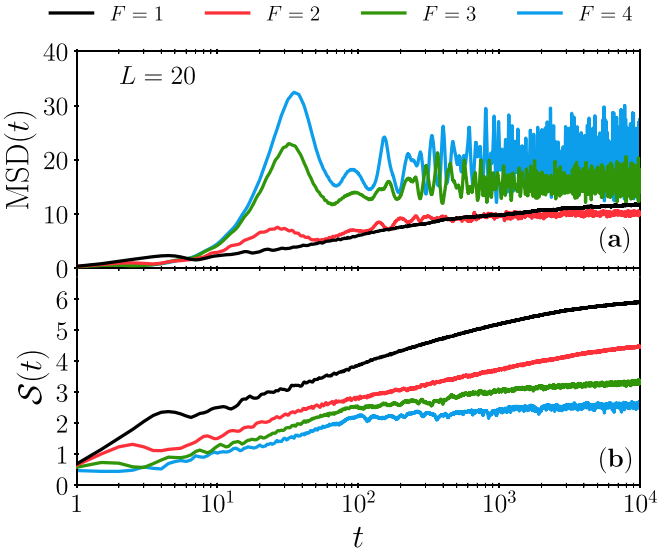

FIG. 7. Long time evolution of MSD in the highly interactive regime ($U = 12$) for different tilts. For small tilts, the mean-square deviation shows a really slow growth followed by a saturation at a small value. When F is large, MSD experiences a fast ramp followed by oscillations around a fixed value.

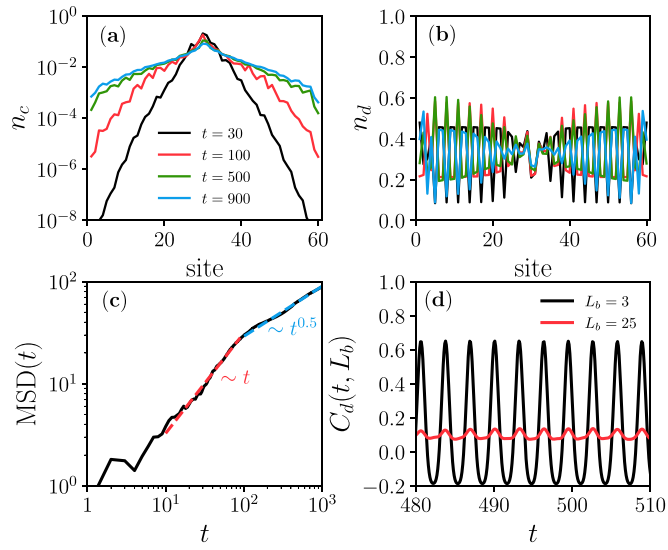

FIG. 8. Time dynamics for $L = 60$ chain. The interaction strength is $U = 12$ and the tilt $F = 2$. The c impurity spreads significantly initially, as seen (a) from the n_c distribution and (c) MSD. The latter plot reveals that, even at long time the spreading is significant. Panel (b) shows the distribution of d particles, delocalized in the middle of the chain but keeping a partial memory of the initial state at larger distances from the center. The correlation function (d) shows significant Bloch oscillations that occurs mainly in the outer regions. The red line traces weak local correlations in the central region.

IV. LARGE SIZES

Larger system sizes require different numerical methods to treat, as exact time evolution requires exponential memory resources. Fortunately, we can use for this purpose a thoroughly tested TDVP algorithm [65,66] which we used in a number of situations involving the dynamics in nonergodic regimes [46,74–78]. We use a combination of single-site and double-site algorithm with dynamically grown auxiliary space dimension up to typically $\chi = 384$. Tests on a number of cases (see the Appendix for more details), and in particular smaller χ, show that we obtain typically below 1% error for local variables (occupation of sites) with a few percent for the entanglement entropy and MSD up to times $t = 1000$ considered. The typical time step used was $dt = 0.05/J$.

Consider first the one-third filling by d particles. The remnants of the impurity localization observed in Fig. 1 could be at first attributed to the small system size, but TDVP evolution of much larger $L = 60$ system (for a considerably shorter time) confirms that quasistationary long-time impurity distribution seems to carry the information about its initial position—compare Fig. 8. The particle seems to spread quite fast for short times with an apparent slowdown around $t \approx 100$, as observed by the time evolution of MSD—Fig. 8(c). While initial growth seems diffusive for later times, $t > 100$, one may fit MSD with a subdiffusive growth, t^α with $\alpha \approx 0.5$. This explains the small difference between c-particle density distributions at late times, as shown in Fig. 8(a). The motion of d particles feeling the tilted lattice is also interesting. The initial density wave distribution of tilted particles significantly evolves in time. One can observe two regions. In the central zone, around the original position of the c boson, the density of d bosons seems to reach the mean 1/3 value apparently loosing any memory of initial occupations. However, moving outside, closer to the edges, the partial memory of the initial distribution persists (except very close to the edges). Comparing data at different times one may observe that the density around the center is almost stationary while in the outside region, Bloch-like oscillations are still visible as could be inferred from Fig. 8(b). This is better visualized by the time-dependent correlation function, Eq. (4). If only the edges are removed by taking $L_b = 3$, Bloch-like oscillations of $C_d(t, 3)$ are quite pronounced. On the other hand for $L_b = 25$, when we measure the correlation function on ten central sites only, the oscillations are to a large extent suppressed as shown in Fig. 8(d). Let us observe also that for the relatively large system, $L = 60$, no apparent asymmetry and accumulation of particles at one edge occurs.

Figure 9 presents the time dynamics of the entanglement entropies at different cuts of the system. Black lines correspond to the central cut at the initial position of the impurity, and red (green) lines correspond to cuts 5 (10) sites to the right, respectively. One clearly observes the delay of the entropy growth, the perturbation induced by the impurity spreads with a finite velocity across the system. Observe that while the configurational part of the entropy grows smoothly the number entropy reveals strong oscillations corresponding to fast Bloch density oscillations. The growth of the entropy is quite significant pointing out towards the spreading of information across the whole system.

The corresponding scenario at $F = 3$ for $L = 60$ is quite similar to the story for small sizes as shown in Fig. 10. The c particle spreads over the whole system revealing, however, traces of localization at the center. Contrary to $F = 2$ case, the density shows a "teeth" structure as the c particle avoids

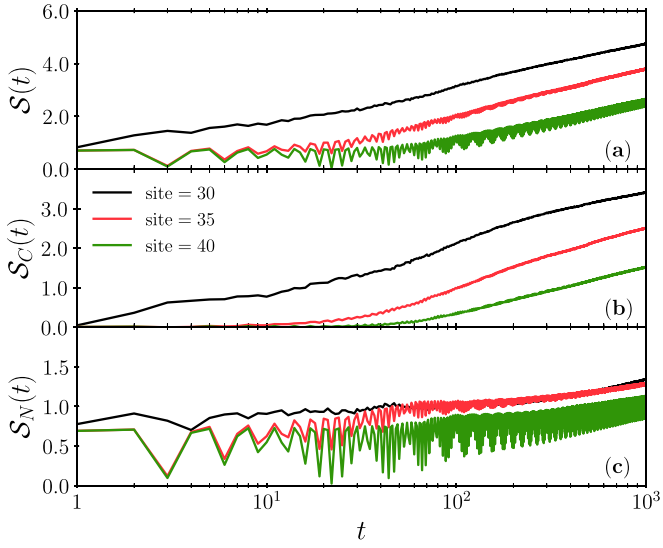

FIG. 9. (a) The time dynamics of the full entanglement entropy, (b) of its quantum (configurational) part S_C, and (c) the classical number entropy S_N, for the same parameters as in Fig. 8, i.e., $U = 12$, $F = 2$. Black, red, and green lines give entropies at the center of the chain at site $i_0 = 30$, at $i_0 + 5$, and $i_0 + 10$, respectively. Observe that the entropy growth is delayed for bonds further from the center. The central bond entropy seems to be growing slightly faster than logarithmically.

sites where d particles are present. Still one may try to fit the exponentially decaying function, $n(i) = A\exp(-B|i - i_0|)$, centered at the initial c-particle position to the long time, $t = 900$, density. The result, on one hand, seems to reproduce the envelope quite well, on the other the numerical density shows small upward trend close to the edges of the chain. Also the resulting "localization length," $1/B \approx 8$ seems quite large showing again that the finite size of the system may affect the distribution. The d particles, on the other hand, are almost frozen

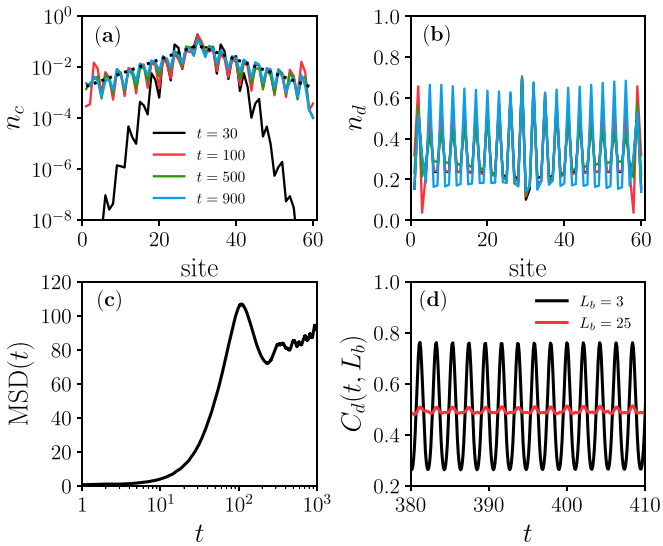

FIG. 10. Same as Fig. 8 but for a larger tilt $F = 3$. Dashed lines in panel (a) represents an attempt at exponential fit of the density $\approx\exp(-B|i - 30|)$ with $B = 0.13$.

in their original positions thus intuition coming from the KP potential seems again applicable. The MSD [Fig. 10(c)] reveals a characteristic small maximum in its initial spread. The later growth as well as the growth of the entanglement entropy (not shown) appears to be logarithmic. Putting all these observations together, this case seems to be very close to being localized. We have no evidence, up to the longest time studied by TDVP, of delocalization of d particles, also the practical freezing of the c-particle distribution and the slow growth of MSD and S points toward this interpretation which cannot be made definitive due to the finite times studied.

Let us now move to the arguably more interesting d-particle half filling case for which more clear signatures of MBL have been observed for small systems. It is particularly interesting in view of a recent study of size dependence of MBL and of its thermodynamic limit. Several works observed a clear shift of MBL threshold with the system size, see, e.g., Refs. [79–82]. It is interesting to see whether the same behavior occurs for our impurity.

In the top row of Fig. 11 the gradual spreading of the c particle may be seen. The fast initial expansion slows considerably for $t > 100$, practically freezing for $F = 2$ or $F = 3$. The $F = 2$ case is particularly interesting with n_c revealing an exponential-like envelope that is as low as 10^{-5} at the edges. For smaller $F = 1$ the spreading is still significant even at late times, while for $F = 3$, localization is clearly weaker reaching around 10^{-3} at the edges. This is reflected in Fig. 11(g), which shows the time dynamics of MSD. Its growth is slowest for $F = 2$, notice also the small (keeping in mind that we consider $L = 60$) value of MSD even at $t = 1000$. For $F = 1$ MSD grows faster while for $F = 3$ it is much larger. The entropy of entanglement seems to grow logarithmically for all F values considered. Still neither $F = 1$ nor $F = 3$ case seems to show features typical for MBL. Thus the slow, logarithmic-like entanglement entropy growth should not be considered as a proof of MBL.

V. THE ROLE OF POSITIONAL DISORDER

Up until now we considered the situation when d particles, feeling the tilted lattice potential, were distributed regularly in the density wave pattern, either $|1, 0, 1, 0, \ldots\rangle$ for half filling or, at the beginning for 1/3-filling, $|0, 1, 0, 0, 1, 0, \ldots\rangle$. In both cases for a strong tilt this structure of the d-particle distribution imitated, to some extend, the KP potential for c particles due to interactions. Instead of the regular density wave pattern, one may consider a random distribution of d particles over the sites. In this way, making d particles for a moment immobile, we create the position-disordered potential for c particle which should then become Anderson localized. Of course, the tunneling of d particles destroys this picture but if the tilt is sufficiently strong, the Stark localization of d particles prevents their tunneling so the c particle sees something approximating a disordered potential. Do we observe MBL in this case?

Indeed this seems to be the case for a strong tilt, $F = 4$, as shown in Fig. 12. We present here results obtained after averaging over 24 realizations of distribution of d particles for 1/3 filling, i.e., for random distribution of 20 d particles on 60 sites. For all the realizations, the c particle was initially

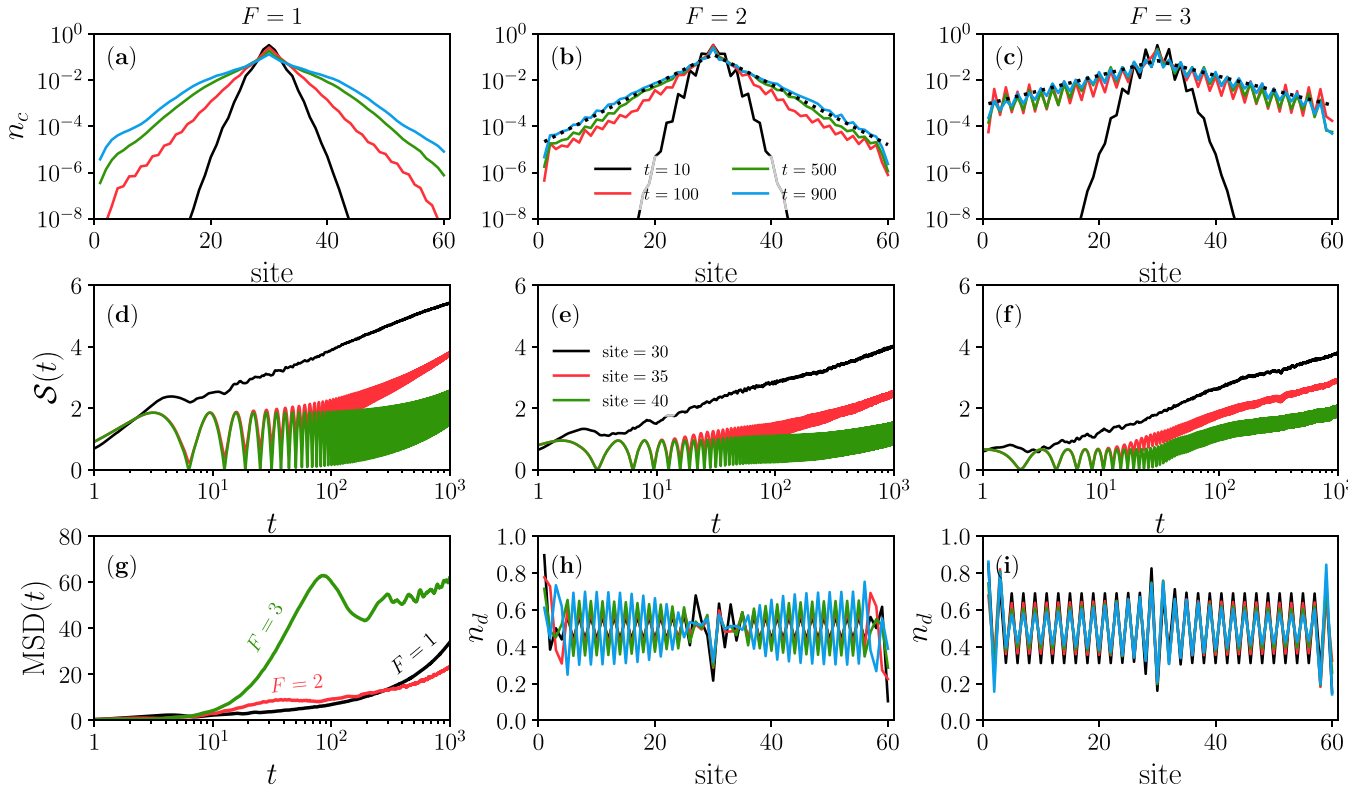

FIG. 11. Time dynamics for half filling by d particles and $U = 12$ case for $F = 1, 2, 3$ as indicated in the panels. Top row [panels (a)–(c)] shows the density of c particles while the middle row [panels (d)–(f)] shows the entanglement entropy at different cuts: in the middle (black), five sites to the right (red) and at site 40 (10 sites from the center, green line). Panel (g) shows MSD for $F = 1$ (black) $F = 2$ (red) and $F = 3$ (green) while panels (h) and (i) show the distribution of d particles for $F = 2$ and $F = 3$ for the same times as in panels (b) and (c). Additionally, panels (b) and (c) show exponential fits to the density $n_c = A\exp(-B|i - i_0|)$ with $B = 0.30$ for $F = 2$ and $B = 0.15$ for $F = 3$.

located at the center at site number 30. We have taken only those random realizations in which this middle site was not occupied by a d particle. This enables a comparison with a density wave scenario where also the central site was not occupied by a d particle.

For $F = 4$ the situation seems very clear. The entanglement entropy reaches a little above unity at final times $t = 1000$ revealing a clear logarithmic growth. Its oscillatory character indicates also that the entanglement entropy is dominated by the number entropy. Similar is the fate of MSD which grows logarithmically. For $F = 2$ it seems, at first glance, that entropy also grows logarithmically, a careful inspection at later times reveals a slightly faster growth. This signature of a long time delocalization is magnified by the behavior of MSD which seems to grow much faster at late times. The correlation of d particles reveals very smooth Bloch-like oscillations, regardless of the random particle distribution which apparently does not affect the regularity of these oscillations.

VI. CONCLUSIONS AND PERSPECTIVES

We have analyzed in detail the behavior of an impurity interacting with other particles that alone would be Wannier-Stark localized due to the lattice tilt. On purpose, we considered a very similar situation to that studied in recent works [44–46,61], where the background particles were Anderson localized.

Analysis of small system sizes, performed by Hamiltonian exponentiation technique [59,60], allowed us to study long-time dynamics. We have shown that, even for strong interactions, comparable to that studied in earlier works on random systems [44–46,61], for a low density of d particles (one-third filling), the resulting dynamics while clearly nonergodic could not be considered as truly many-body localized. On the other hand, for the optimal one-half density, when the interactions are effectively maximized, clear manifestations of MBL were observed, e.g., via the slow logarithmic growth of the entanglement entropy or of the mean squared deviation of c-particle distribution.

We have observed an interesting effect absent in the random-localized case and present here for significant interspecies interaction strength U and a sufficiently large tilt, F. Such a tilt makes the Wannier-Stark localization length (and the amplitude of Bloch oscillations) very small, much smaller than the lattice spacings. This pins down d particles to their original positions and they generate an effective potential for c particles. For regular distribution of d-particles the resulting potential is periodic resembling Kronig-Penney potential and c particles spreads in it. Interestingly, at later times the distribution reveals some signature of stabilization (with large fluctuations of MSD) accompanied by a logarithmic in time entropy growth. This suggests localization.

The results for small systems were fully confirmed with tensor network TDVP numerical calculations that could be

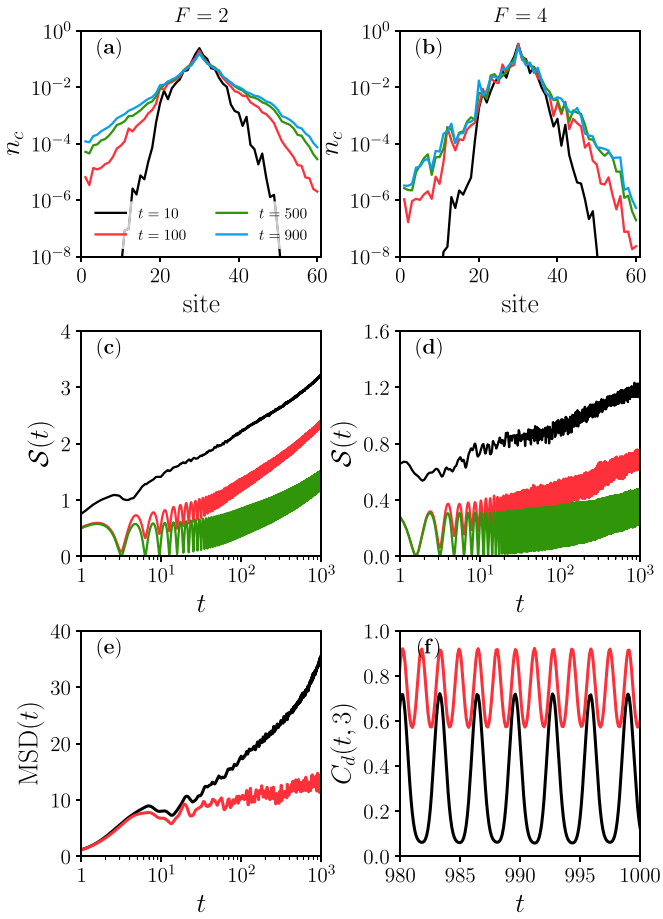

FIG. 12. Time dynamics for 1/3 filling (randomly distributed d bosons), $U = 12$ case for $F = 2$ (left column) and $F = 4$ (right column). Strong exponential-like localization of c boson (top row) is observed. It is accompanied by (d) a log growth of the entanglement entropy and a similar growth of MSD [panel (e), red line] for $F = 4$. (c) For $F = 2$ entanglement entropy grows slightly faster than logarithmically, also MSD grows faster, indicating lack of localization in that case. As in the previous figure we show the entropies at three different bonds: in the middle position i_0 and at $i_0 + 5$. $i_0 + 10$ to visualize spreading of entanglement in the system. Panel (f) shows correlations of d bosons which remain very large and reveal fast Bloch oscillations.

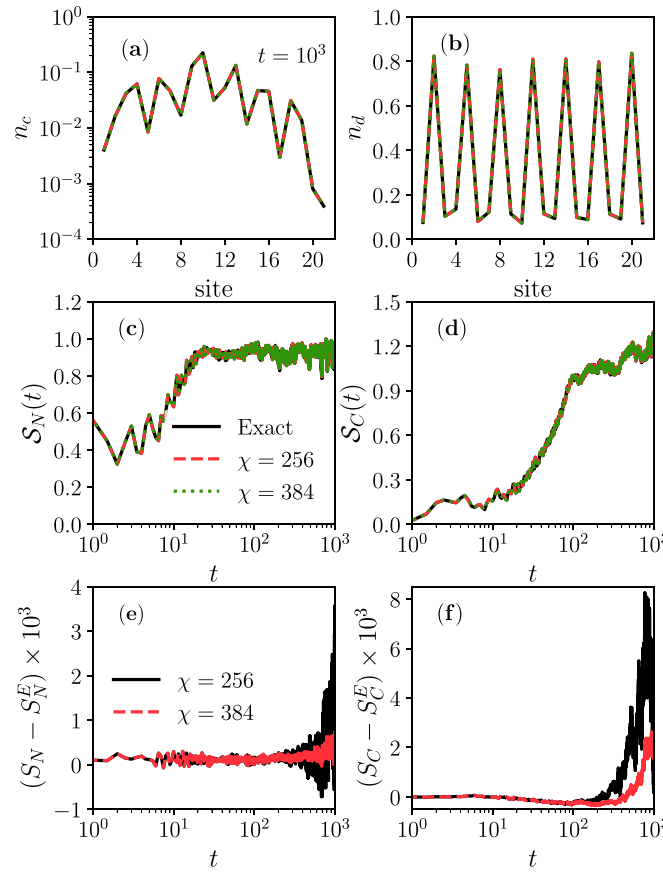

FIG. 13. Comparison of time dynamics obtained with Hamiltonian exponentiation with results of TDVP algorithm for $L = 21$, $F = 4, U = 12$. Top row shows the occupations of sites for the impurity (left) and d particles. The agreement is spectacular. The middle row shows the number and configurational parts of the entanglement entropy. Their errors (note the change of the vertical scale) are shown in the bottom row.

carried out up to 1000 tunneling times (i.e., well below current experimental capabilities [50]). The fact that the calculations could reach such long times indicates limited entanglement build-up and localized character of observed distributions.

The situation dramatically changes for a random distribution of d particles in the tilted potential. Then for large tilt, they form a random potential due to their random positions. The coupled evolution of the full system shows then much stronger signatures of MBL with much slower entanglement entropy growth as well as an extremely slow spread of the c particle density. Clearly, such a combination of a strong tilt and random particle distribution leads to robust many-body localization.

This suggests that even in the absence of a tilt one could observe MBL more clearly in the random case as the one studied in Refs. [44–46,61]. One needs then sufficiently strong disorder to have the Anderson localization length of the order of the lattice site spacing for d particles but, importantly, they should be randomly and not regularly (as in Refs. [44–46,61]) distributed. A study in this direction is in progress.

ACKNOWLEDGMENTS

We are grateful to K. Sacha and P. Sierant for enlightening discussions, to O. Readon-Smith for critical remarks as well as to A. Sai Aramthottil for useful hints on numerics. J.Z. is supported by the National Science Centre (Poland) under Grant No. OPUS18 2019/35/B/ST2/00034. The work of PRNF was funded by the National Science Centre, Poland, Project No. 2021/03/Y/ST2/00186 within the QuantERA II Programme that has received funding from the European Union Horizon 2020 research and innovation programme under Grant Agreement No. 101017733. We gratefully acknowledge the Polish high-performance computing infrastructure PLGrid (HPC Centers: ACK Cyfronet AGH) for providing computer facilities and support within computational Grant No. PLG/2022/015613. Views and opinions expressed in this work are, however, those of the author(s) only and do not

necessarily reflect those of the European Union, European Climate, Infrastructure and Environment Executive Agency (CINEA), nor any other granting authority. Neither the European Union nor any granting authority can be held responsible for them. Authors declare that they did not involve any artificial intelligence tool in writing this paper.

APPENDIX

We provide here more details on the TDVP algorithm and its application to the problem studied. The foundation of the method as well as details of its implementation may be found, e.g., in a recent review [65]. We mention that our implementation has been tested already in several numerical studies of dynamics in many-body systems, in particular, those related to MBL [46,53–55,74–77].

In numerical studies performed in this study we use a hybrid version of TDVP [65,66]. At the initial stage it uses a two-site version of TDVP. The initial state is represented as a matrix product state (since we start the time evolution from product states this is straightforward). During the time evolution the auxiliary bond dimension grows reflecting the buildup of the entanglement in the system. We assume some maximal allowed bond dimension χ and the evolution is followed with the two-site version until this value of χ is reached. Then we switch to the single-site version. That allows us to partially avoid errors related to the truncation of the singular values in the two-site version [65,66]. Controlling the errors related to a necessary restriction of the Hilbert-space dimension as well as comparing the results for different χ allows us to assess the convergence of the results.

A comparison of the TDVP performance with the "exact" results may be carried out for small system sizes only. Figure 13 shows such a comparison for the $F = 4$, $U = 12$ system for $L = 21$. In the whole time interval studied the agreement is highly satisfactory, the curves resulting from the exact and TDVP evolution practically coincide. In fact, the occupation of sites is not a very sensitive measure of this agreement, more details are provided by comparison of time dynamics of entropies. As shown in the bottom row of Fig. 13 some differences between exact entropies and those obtained using TDVP are visible for late times. Still even for the largest time considered, $t = 1000$ the errors for $\chi = 256$ are below 1%, being about six times smaller for $\chi = 384$. For larger system sizes no comparison with "quasi-exact" time dynamics is possible so we could compare the results of simulations for different χ only. A comparison with smaller χ results showed small differences (for entropies) at large times, differences that did not affect the conclusions presented.

We must note, at the same time, that large values of U and F made the TDVP algorithm very costly in the execution time. Some of the data presented required about two weeks of single-processor time. Our version of TDVP uses a typical for standard density matrix renormalization group (DMRG) technique of sweeping along the chain that prevented us from an otherwise possible parallelization of the algorithm.

[1] L. D. Landau, Electron motion in crystal lattices, Phys. Z. Sowjet. **3**, 664 (1933).
[2] S. I. Pekar, Local quantum states of electrons in an ideal ion crystal, Zh. Eksp. Teor. Phys. **16**, 341 (1946).
[3] S. I. Pekar, Theory of colored crystals, Zh. Eksp. Teor. Phys. **17**, 868 (1947).
[4] S. I. Pekar, Novel view on electron conductance of ion crystals, Zh. Eksp. Teor. Phys. **18**, 105 (1948).
[5] L. Landau and S. I. Pekar, Effective mass of a polaron, Zh. Eksp. Teor. Phys. **18**, 419 (1948).
[6] R. Côté, V. Kharchenko, and M. D. Lukin, Mesoscopic molecular ions in Bose-Einstein condensates, Phys. Rev. Lett. **89**, 093001 (2002).
[7] P. Massignan, C. J. Pethick, and H. Smith, Static properties of positive ions in atomic Bose-Einstein condensates, Phys. Rev. A **71**, 023606 (2005).
[8] F. M. Cucchietti and E. Timmermans, Strong-coupling polarons in dilute gas Bose-Einstein condensates, Phys. Rev. Lett. **96**, 210401 (2006).
[9] S. Palzer, C. Zipkes, C. Sias, and M. Köhl, Quantum transport through a Tonks-Girardeau gas, Phys. Rev. Lett. **103**, 150601 (2009).
[10] J. Catani, G. Lamporesi, D. Naik, M. Gring, M. Inguscio, F. Minardi, A. Kantian, and T. Giamarchi, Quantum dynamics of impurities in a one-dimensional Bose gas, Phys. Rev. A **85**, 023623 (2012).
[11] N. Spethmann, F. Kindermann, S. John, C. Weber, D. Meschede, and A. Widera, Dynamics of single neutral impurity atoms immersed in an ultracold gas, Phys. Rev. Lett. **109**, 235301 (2012).
[12] J. Bonart and L. F. Cugliandolo, From nonequilibrium quantum Brownian motion to impurity dynamics in one-dimensional quantum liquids, Phys. Rev. A **86**, 023636 (2012).
[13] S. P. Rath and R. Schmidt, Field-theoretical study of the Bose polaron, Phys. Rev. A **88**, 053632 (2013).
[14] T. Fukuhara, A. Kantian, M. Endres, M. Cheneau, P. Schauß, S. Hild, D. Bellem, U. Schollwöck, T. Giamarchi, C. Gross, I. Bloch, and S. Kuhr, Quantum dynamics of a mobile spin impurity, Nat. Phys. **9**, 235 (2013).
[15] A. Shashi, F. Grusdt, D. A. Abanin, and E. Demler, Radio-frequency spectroscopy of polarons in ultracold Bose gases, Phys. Rev. A **89**, 053617 (2014).
[16] F. Meinert, M. Knap, E. Kirilov, K. Jag-Lauber, M. B. Zvonarev, E. Demler, and H.-C. Nägerl, Bloch oscillations in the absence of a lattice, Science **356**, 945 (2017).
[17] A. Schirotzek, C.-H. Wu, A. Sommer, and M. W. Zwierlein, Observation of Fermi polarons in a tunable fermi liquid of ultracold atoms, Phys. Rev. Lett. **102**, 230402 (2009).
[18] S. Nascimbène, N. Navon, K. J. Jiang, L. Tarruell, M. Teichmann, J. McKeever, F. Chevy, and C. Salomon, Collective oscillations of an imbalanced fermi gas: Axial compression modes and polaron effective mass, Phys. Rev. Lett. **103**, 170402 (2009).
[19] A. Sommer, M. Ku, and M. W. Zwierlein, Spin transport in polaronic and superfluid Fermi gases, New J. Phys. **13**, 055009 (2011).

[20] C. Kohstall, M. Zaccanti, M. Jag, A. Trenkwalder, P. Massignan, G. M. Bruun, F. Schreck, and R. Grimm, Metastability and coherence of repulsive polarons in a strongly interacting Fermi mixture, Nature (London) **485**, 615 (2012).

[21] B. Fröhlich, M. Feld, E. Vogt, M. Koschorreck, W. Zwerger, and M. Köhl, Radio-frequency spectroscopy of a strongly interacting two-dimensional Fermi gas, Phys. Rev. Lett. **106**, 105301 (2011).

[22] M. Koschorreck, D. Pertot, E. Vogt, B. Fröhlich, M. Feld, and M. Köhl, Attractive and repulsive Fermi polarons in two dimensions, Nature (London) **485**, 619 (2012).

[23] P. Massignan, M. Zaccanti, and G. M. Bruun, Polarons, dressed molecules and itinerant ferromagnetism in ultracold Fermi gases, Rep. Prog. Phys. **77**, 034401 (2014).

[24] Z. Yan, P. B. Patel, B. Mukherjee, R. J. Fletcher, J. Struck, and M. W. Zwierlein, Boiling a unitary Fermi liquid, Phys. Rev. Lett. **122**, 093401 (2019).

[25] M.-G. Hu, M. J. Van de Graaff, D. Kedar, J. P. Corson, E. A. Cornell, and D. S. Jin, Bose polarons in the strongly interacting regime, Phys. Rev. Lett. **117**, 055301 (2016).

[26] N. B. Jørgensen, L. Wacker, K. T. Skalmstang, M. M. Parish, J. Levinsen, R. S. Christensen, G. M. Bruun, and J. J. Arlt, Observation of attractive and repulsive polarons in a Bose-Einstein condensate, Phys. Rev. Lett. **117**, 055302 (2016).

[27] Z. Z. Yan, Y. Ni, C. Robens, and M. W. Zwierlein, Bose polarons near quantum criticality, Science **368**, 190 (2020).

[28] C. J. M. Mathy, M. B. Zvonarev, and E. Demler, Quantum flutter of supersonic particles in one-dimensional quantum liquids, Nat. Phys. **8**, 881 (2012).

[29] M. Schecter, A. Kamenev, D. M. Gangardt, and A. Lamacraft, Critical velocity of a mobile impurity in one-dimensional quantum liquids, Phys. Rev. Lett. **108**, 207001 (2012).

[30] F. Massel, A. Kantian, A. J. Daley, T. Giamarchi, and P. Törmä, Dynamics of an impurity in a one-dimensional lattice, New J. Phys. **15**, 045018 (2013).

[31] C. Charalambous, M. A. Garcia-March, A. Lampo, M. Mehboud, and M. Lewenstein, Two distinguishable impurities in BEC: Squeezing and entanglement of two Bose polarons, SciPost Phys. **6**, 010 (2019).

[32] C. Charalambous, M. Á. García-March, G. Muñoz-Gil, P. R. Grzybowski, and M. Lewenstein, Control of anomalous diffusion of a Bose polaron, Quantum **4**, 232 (2020).

[33] A. Lampo, S. H. Lim, M. Á. García-March, and M. Lewenstein, Bose polaron as an instance of quantum Brownian motion, Quantum **1**, 30 (2017).

[34] M. Mehboudi, A. Lampo, C. Charalambous, L. A. Correa, M. A. García-March, and M. Lewenstein, Using polarons for sub-nK quantum nondemolition thermometry in a Bose-Einstein condensate, Phys. Rev. Lett. **122**, 030403 (2019).

[35] M. M. Khan, H. Terças, J. T. Mendonça, J. Wehr, C. Charalambous, M. Lewenstein, and M. A. Garcia-March, Quantum dynamics of a Bose polaron in a d-dimensional Bose-Einstein condensate, Phys. Rev. A **103**, 023303 (2021).

[36] M. M. Khan, M. Mehboudi, H. Terças, M. Lewenstein, and M. A. Garcia-March, Subnanokelvin thermometry of an interacting d-dimensional homogeneous Bose gas, Phys. Rev. Res. **4**, 023191 (2022).

[37] L. D'Alessio, Y. Kafri, A. Polkovnikov, and M. Rigol, From quantum chaos and eigenstate thermalization to statistical mechanics and thermodynamics, Adv. Phys. **65**, 239 (2016).

[38] J. Bonča and M. Mierzejewski, Delocalized carriers in the $t-j$ model with strong charge disorder, Phys. Rev. B **95**, 214201 (2017).

[39] S. Gopalakrishnan, K. R. Islam, and M. Knap, Noise-induced subdiffusion in strongly localized quantum systems, Phys. Rev. Lett. **119**, 046601 (2017).

[40] G. Lemut, M. Mierzejewski, and J. Bonča, Complete many-body localization in the $t-j$ model caused by a random magnetic field, Phys. Rev. Lett. **119**, 246601 (2017).

[41] J. Bonča, S. A. Trugman, and M. Mierzejewski, Dynamics of the one-dimensional Anderson insulator coupled to various bosonic baths, Phys. Rev. B **97**, 174202 (2018).

[42] P. Prelovšek, J. Bonča, and M. Mierzejewski, Transient and persistent particle subdiffusion in a disordered chain coupled to bosons, Phys. Rev. B **98**, 125119 (2018).

[43] U. Krause, T. Pellegrin, P. W. Brouwer, D. A. Abanin, and M. Filippone, Nucleation of ergodicity by a single mobile impurity in supercooled insulators, Phys. Rev. Lett. **126**, 030603 (2021).

[44] P. Brighi, A. A. Michailidis, D. A. Abanin, and M. Serbyn, Propagation of many-body localization in an Anderson insulator, Phys. Rev. B **105**, L220203 (2022).

[45] P. Brighi, A. A. Michailidis, K. Kirova, D. A. Abanin, and M. Serbyn, Localization of a mobile impurity interacting with an Anderson insulator, Phys. Rev. B **105**, 224208 (2022).

[46] P. Sierant, T. Chanda, M. Lewenstein, and J. Zakrzewski, Slow dynamics of a mobile impurity interacting with an Anderson insulator, Phys. Rev. B **107**, 144201 (2023).

[47] E. van Nieuwenburg, Y. Baum, and G. Refael, From Bloch oscillations to many-body localization in clean interacting systems, Proc. Natl. Acad. Sci. USA **116**, 9269 (2019).

[48] M. Schulz, C. A. Hooley, R. Moessner, and F. Pollmann, Stark many-body localization, Phys. Rev. Lett. **122**, 040606 (2019).

[49] S. R. Taylor, M. Schulz, F. Pollmann, and R. Moessner, Experimental probes of Stark many-body localization, Phys. Rev. B **102**, 054206 (2020).

[50] S. Scherg, T. Kohlert, P. Sala, F. Pollmann, B. H. Madhusudhana, I. Bloch, and M. Aidelsburger, Observing nonergodicity due to kinetic constraints in tilted Fermi-Hubbard chains, Nat. Commun. **12**, 4490 (2021).

[51] Q. Guo, C. Cheng, H. Li, S. Xu, P. Zhang, Z. Wang, C. Song, W. Liu, W. Ren, H. Dong, R. Mondaini, and H. Wang, Stark many-body localization on a superconducting quantum processor, Phys. Rev. Lett. **127**, 240502 (2021).

[52] W. Morong, F. Liu, P. Becker, K. S. Collins, L. Feng, A. Kyprianidis, G. Pagano, T. You, A. V. Gorshkov, and C. Monroe, Observation of Stark many-body localization without disorder, Nature (London) **599**, 393 (2021).

[53] R. Yao and J. Zakrzewski, Many-body localization of bosons in an optical lattice: Dynamics in disorder-free potentials, Phys. Rev. B **102**, 104203 (2020).

[54] R. Yao, T. Chanda, and J. Zakrzewski, Many-body localization in tilted and harmonic potentials, Phys. Rev. B **104**, 014201 (2021).

[55] R. Yao, T. Chanda, and J. Zakrzewski, Nonergodic dynamics in disorder-free potentials, Ann. Phys. (NY) **435**, 168540 (2021).

[56] E. V. H. Doggen, I. V. Gornyi, and D. G. Polyakov, Stark many-body localization: Evidence for Hilbert-space shattering, Phys. Rev. B **103**, L100202 (2021).

[57] V. Oganesyan and D. A. Huse, Localization of interacting fermions at high temperature, Phys. Rev. B **75**, 155111 (2007).

[58] Y. Y. Atas, E. Bogomolny, O. Giraud, and G. Roux, Distribution of the ratio of consecutive level spacings in random matrix ensembles, Phys. Rev. Lett. **110**, 084101 (2013).
[59] P. Weinberg and M. Bukov, QuSpin: A Python package for dynamics and exact diagonalisation of quantum many body systems part I: spin chains, SciPost Phys. **2**, 003 (2017).
[60] P. Weinberg and M. Bukov, QuSpin: A Python package for dynamics and exact diagonalisation of quantum many body systems. Part II: bosons, fermions and higher spins, SciPost Phys. **7**, 020 (2019).
[61] P. Brighi, M. Ljubotina, D. A. Abanin, and M. Serbyn, Many-body localization proximity effect in two-species bosonic Hubbard model, Phys. Rev. B **108**, 054201 (2023).
[62] C. N. Varney, K. Sun, V. Galitski, and M. Rigol, Quantum phases of hard-core bosons in a frustrated honeycomb lattice, New J. Phys. **14**, 115028 (2012).
[63] H.-K. Wu and W.-L. Tu, Competing quantum phases of hard-core bosons with tilted dipole-dipole interaction, Phys. Rev. A **102**, 053306 (2020).
[64] W.-H. Li, X. Deng, and L. Santos, Hilbert space shattering and disorder-free localization in polar lattice gases, Phys. Rev. Lett. **127**, 260601 (2021).
[65] S. Paeckel, T. Köhler, A. Swoboda, S. R. Manmana, U. Schollwöck, and C. Hubig, Time-evolution methods for matrix-product states, Ann. Phys. (NY) **411**, 167998 (2019).
[66] S. Goto and I. Danshita, Performance of the time-dependent variational principle for matrix product states in the long-time evolution of a pure state, Phys. Rev. B **99**, 054307 (2019).
[67] S. Bera, G. De Tomasi, F. Weiner, and F. Evers, Density propagator for many-body localization: Finite-size effects, transient subdiffusion, and exponential decay, Phys. Rev. Lett. **118**, 196801 (2017).
[68] F. Weiner, F. Evers, and S. Bera, Slow dynamics and strong finite-size effects in many-body localization with random and quasiperiodic potentials, Phys. Rev. B **100**, 104204 (2019).
[69] I. Bengtsson and K. Życzkowski, *Geometry of Quantum States: An Introduction to Quantum Entanglement* (Cambridge University Press, Cambridge, 2006).
[70] A. Lukin, M. Rispoli, R. Schittko, M. E. Tai, A. M. Kaufman, S. Choi, V. Khemani, J. Léonard, and M. Greiner, Probing entanglement in a many-body–localized system, Science **364**, 256 (2019).
[71] M. Žnidarič, T. Prosen, and P. Prelovšek, Many-body localization in the Heisenberg XXZ magnet in a random field, Phys. Rev. B **77**, 064426 (2008).
[72] J. H. Bardarson, F. Pollmann, and J. E. Moore, Unbounded growth of entanglement in models of many-body localization, Phys. Rev. Lett. **109**, 017202 (2012).
[73] C. Kittel, *Introduction to Solid State Physics* (John Wiley and Sons, Hoboken, 2005).
[74] T. Chanda, J. Zakrzewski, M. Lewenstein, and L. Tagliacozzo, Confinement and lack of thermalization after quenches in the bosonic Schwinger model, Phys. Rev. Lett. **124**, 180602 (2020).
[75] T. Chanda, P. Sierant, and J. Zakrzewski, Time dynamics with matrix product states: Many-body localization transition of large systems revisited, Phys. Rev. B **101**, 035148 (2020).
[76] T. Chanda, R. Yao, and J. Zakrzewski, Coexistence of localized and extended phases: Many-body localization in a harmonic trap, Phys. Rev. Res. **2**, 032039(R) (2020).
[77] T. Chanda, P. Sierant, and J. Zakrzewski, Many-body localization transition in large quantum spin chains: The mobility edge, Phys. Rev. Res. **2**, 032045(R) (2020).
[78] P. Sierant and J. Zakrzewski, Challenges to observation of many-body localization, Phys. Rev. B **105**, 224203 (2022).
[79] J. Šuntajs, J. Bonča, T. Prosen, and L. Vidmar, Ergodicity breaking transition in finite disordered spin chains, Phys. Rev. B **102**, 064207 (2020).
[80] J. Šuntajs, J. Bonča, T. Prosen, and L. Vidmar, Quantum chaos challenges many-body localization, Phys. Rev. E **102**, 062144 (2020).
[81] P. Sierant, D. Delande, and J. Zakrzewski, Thouless time analysis of anderson and many-body localization transitions, Phys. Rev. Lett. **124**, 186601 (2020).
[82] P. Sierant, M. Lewenstein, and J. Zakrzewski, Polynomially filtered exact diagonalization approach to many-body localization, Phys. Rev. Lett. **125**, 156601 (2020).